ELECTROWEAK MEASUREMENTS WITH THE CMS DETECTOR*

V. Ciulli

on behalf of the CMS Collaboration

Dipartimento di Fisica, Università di Firenze and INFN Firenze
via G. Sansone 1, 50019, Sesto Fiorentino, Italy
vitaliano.ciulli@unifi.it

(Received May 6, 2020)

Electroweak measurements are at the core of the Large Hadron Collider physics program. The most recent results obtained by the CMS experiment with Drell–Yan, W and multi-boson events will be reviewed. These include the measurement of the electroweak mixing angle, the differential distributions in Drell–Yan events, electroweak production of one and two vector bosons in association with two jets. No deviations from the Standard Model predictions are found and stringent bounds are set on anomalous triple and quartic gauge couplings.

DOI:10.5506/APhysPolB.51.1315

1. Introduction

Electroweak (EW) processes, involving the production or exchange of weak vector bosons and photons, are one of the most important characteristics of the Standard Model (SM) theory of particle interactions. They are at the heart of the Higgs mechanism that allows to give a mass to all fundamental particles and since their discovery they have been studied in great details at all particle colliders including the Large Hadron Collider (LHC) at CERN.

The CMS experiment is one of the two general purpose experiments at the LHC. The central feature of the CMS apparatus is a superconducting solenoid of 6 m internal diameter, providing a magnetic field of 3.8 T.

* Presented at XXVI Cracow Epiphany Conference on LHC Physics: Standard Model and Beyond, Kraków, Poland, January 7–10, 2020.

Within the solenoid volume there are a silicon pixel and strip tracker, a lead tungstate crystal electromagnetic calorimeter, and a brass and scintillator hadron calorimeter, each composed of a barrel and two endcap sections. Forward calorimeters extend the pseudorapidity coverage provided by the barrel and endcap detectors. Muons are detected in gas-ionization chambers embedded in the steel flux-return yoke outside the solenoid. A more detailed description of the CMS detector, together with a definition of the coordinate system used and the relevant kinematic variables, can be found in Ref. [1].

In about ten years since the starting of operations, CMS has collected data of proton–proton collisions at different center-of-mass energies, from 7 TeV to 13 TeV, for a total integrated luminosity of about 200 fb^{-1}. In particular, about 160 fb^{-1} have been taken between 2015 and 2018 at 13 TeV, during the LHC Run 2 period, and an additional 300 fb^{-1} at a similar energy are expected from Run 3 between 2021 and 2024.

Using these data, EW processes with cross-section values ranging over more than nine orders of magnitude have been investigated: from single vector boson production down to triple W bosons and vector boson scattering. In the following, the most recent results are reported.

2. Drell–Yan measurements

Vector bosons allow precision measurements of fundamental parameters through their couplings to fermions. In proton–proton collisions, single W and Z are mainly generated by the annihilation of a valence quark and a sea anti-quark. At the LHC, however, given that the parton energy fractions corresponding to $Q \approx 100$ GeV are in the range of $10^{-3} \div 10^{-1}$, sea–sea contributions are also important. Furthermore, at next-to-leading-order in QCD (NLO), the associated production of a vector boson and jet depends also on the gluon parton distribution function (PDF). Therefore, most EW measurements will strongly depend on PDFs.

At 13 TeV center-of-mass energy, the Drell–Yan (DY) differential cross section *versus* dilepton mass has been measured by CMS between 15 GeV and 3 TeV [2]. Results are given both in a fiducial region and acceptance corrected. Dimuon and dielectron are combined after corrections are applied for the resolution effects and final-state QED radiation. The uncertainty in the measurement is dominated by the statistical error in the high dilepton mass region, and by the systematic error in the acceptance, mostly related to the PDF, in the low-mass region. Figure 1 shows a comparison of the full phase-space results to the next-to-next-leading-order (NNLO) predictions from FEWZ [3]. Overall, there is an excellent agreement with theoretical calculations.

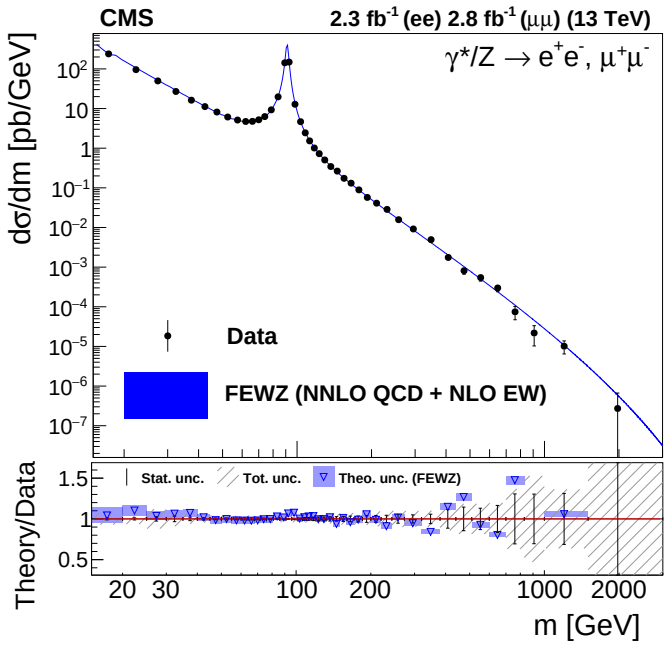

Fig. 1. (Color online) The differential DY cross section measured for the combination of the two channels and as predicted by the NNLO theoretical calculation of FEWZ in the full phase space. The ratio between the data and the theoretical prediction is presented in the bottom panel. The colored boxes represent the theoretical uncertainties [2].

The differential cross sections for the production of a Z boson *versus* the dilepton transverse momentum p_{T}, the rapidity, and the $\phi*$ angle have been also measured at 13 TeV [4]. Results are compared with many theoretical predictions, including parton shower Monte Carlo, resummed and NNLO fixed calculations, showing overall a good agreement within the accuracy of the different predictions.

The angular distribution of the leptons in the DY process has been used to measure the value of the weak mixing angle with proton–proton data at 8 TeV [5]. The interference between the axial and vector current at the Z pole determines the forward–backward asymmetry A_{FB} of the lepton with respect to the direction of the incoming quark, from which, therefore, it is possible to extract $\sin^2\theta^{\ell}_{\mathrm{eff}}$. The direction of the incoming quark is estimated from the boost of the dilepton system, since valence quarks tend to have a larger parton fraction x than antiquarks from the sea. This assumption leads to a dilution of the asymmetry that is strongly dependent on the dilepton rapidity, having a higher probability to be true for larger values of

the boost. The measurement is also very sensitive to the relative amount of up- and down-type quarks in the PDFs. These are, however, constrained using the measured dependence of A_{FB} on the dilepton mass: outside of the Z peak, the A_{FB} is dominated by the interference between Z and γ^* s-channel diagrams and, therefore, depends on the quark charge. This is illustrated in figure 2 where the sensitivity to the $\sin^2\theta^{\ell}_{\mathrm{eff}}$ and the PDF uncertainty are shown *versus* the dilepton mass in different regions of the dilepton rapidity. The result of the fit is shown in figure 3. The measurement yields a value of $\sin^2\theta^{\ell}_{\mathrm{eff}} = 0.23101 \pm 0.00036(\mathrm{stat.}) \pm 0.00018(\mathrm{syst.}) \pm 0.00016(\mathrm{theor.}) \pm 0.00031(\mathrm{PDF})$, which agrees with the average of LEP and SLD results $\sin^2\theta^{\ell}_{\mathrm{eff}} = 0.23153 \pm 0.00016$. The uncertainty is still more than three times larger, but with additional statistics and combined with other measurements from hadron colliders, it can help in the future to disentangle the long-standing LEP/SLD tension [6].

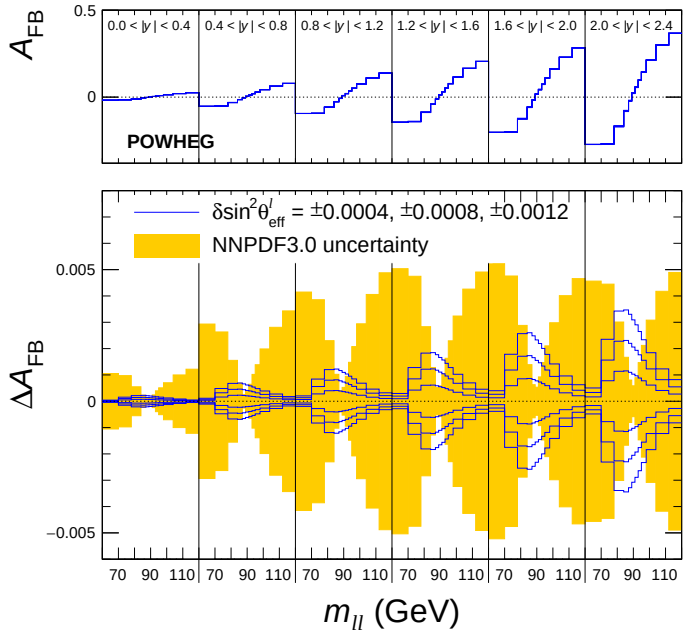

Fig. 2. Distribution in A_{FB} as a function of dilepton mass, in six rapidity bins for $\sin^2\theta^{\ell}_{\mathrm{eff}} = 0.23120$ in POWHEG [7]. The solid lines in the bottom panel correspond to six changes at $\sin^2\theta^{\ell}_{\mathrm{eff}}$ around the central value, corresponding to: ±0.00040, ±0.00080, and ±0.00120. The shaded bands illustrate the standard deviation in the NNPDF3.0 [8] replicas.

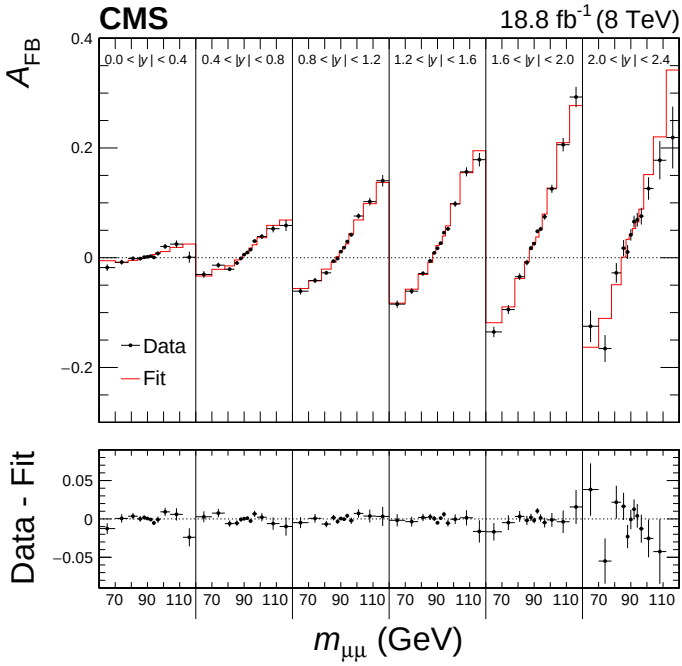

Fig. 3. Comparison between data and best-fit A_{FB} distributions in the dimuon channel. The error bars represent the statistical uncertainties in the data [5].

3. Multi-boson processes

Processes involving two or more vector bosons have cross sections which can be many orders of magnitude lower than single-boson production. Depending on the final state, diboson production is in the range of 5–300 pb, triboson production and Vector Boson Fusion (VBF) are below 1 pb, and Vector Boson Scattering (VBS) is in the range of 0.1–10 fb. In addition, to providing a stringent test of SM electroweak interactions, measurements of these processes allow for searches of New Physics beyond the SM, because triple and quartic gauge couplings (abbreviated, respectively, as TGC and QGC) are especially sensitive to new fields. The theoretical framework most commonly employed in recent times to look for deviations from the SM is the effective field theory (EFT) [9, 10]. Most of the measurements that are presented below provide important constraints on coefficients of dimension-6 and dimension-8 operators, usually from the distributions at high values of the bosons p_{T}. Here, only some of these results can be highlighted. The interested reader is invited to look at the references for the complete set of results.

3.1. Electroweak production of a W boson and two jets

The electroweak production of a vector boson and two jets, which includes vector boson fusion, is of special interest being topologically very similar to VBS. This final state is difficult to disentangle from the overwhelming QCD background of vector boson production in association with two jets. The large rapidity separation and high invariant mass of the tagging jets are a clear signature, but that is not sufficient. For the measurement of electroweak Wjj production at 13 TeV [11], these have been combined in a boosted decision tree (BDT) with the lepton Zeppenfeld variable z^* and a quark–gluon discriminator. Thanks to the discriminating power of this BDT, a sample enriched in 42% signal content is selected. The measured cross section is $\sigma_{\mathrm{EW}}(Wjj) = 6.23 \pm 0.12(\mathrm{stat.}) \pm 0.61(\mathrm{syst.})$ pb, corresponding to a signal strength, *i.e.* a ratio to the SM prediction, of $\mu = 0.91 \pm 0.10$. The additional hadronic activity of events in this signal-enriched region is also studied being an observable very sensitive to the color flow in this particular event topology: in figure 4, the p_{T} of the third jet is compared with prediction from Herwig++ [12], showing a remarkable agreement.

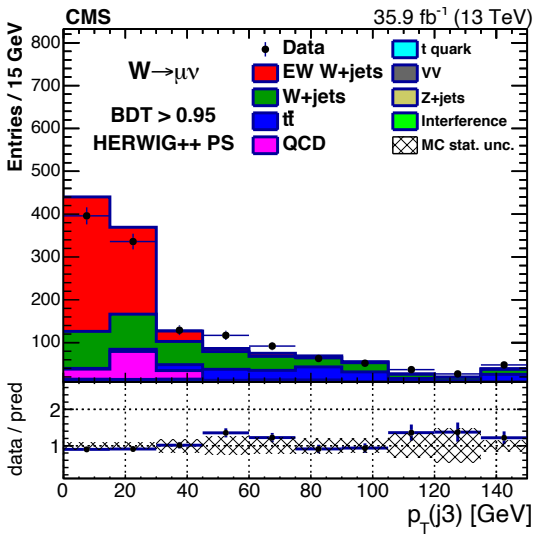

Fig. 4. Leading additional jet p_{T} for BDT > 0.95 in the muon channel including signal with Herwig++ parton showering. The first bin contains events where no additional jet with $p_{\mathrm{T}} > 15$ GeV is present and the last bin contains overflows [11].

3.2. Multi-boson production

Using the 13 TeV dataset, the multi-boson production has been measured in many different channels. A preliminary measurement on the full Run 2 dataset is available for the production of ZZ pairs decaying fully leptonically [13]. In figure 5, results at different center-of-mass energies are compared with theoretical predictions, showing a much better agreement for NNLO predictions from MATRIX [14] than for NLO from MFCM [15].

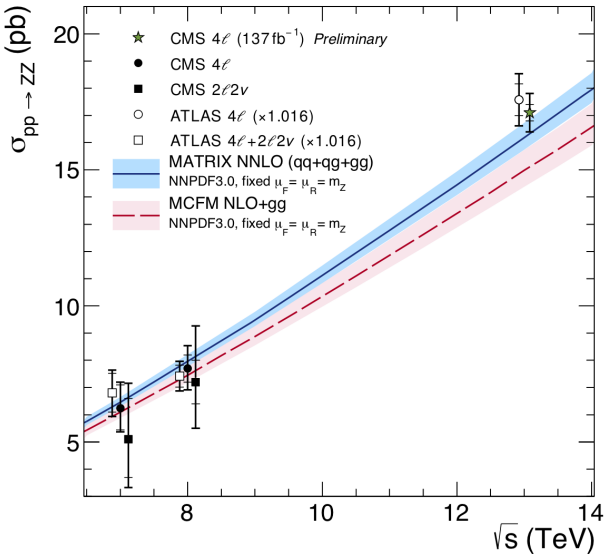

Fig. 5. The total ZZ cross section as a function of the proton–proton center-of-mass energy [13]. The ATLAS measurements were performed with a ZZ boson mass window of 66–116 GeV, instead of 60–120 GeV used by CMS, and are corrected for the resulting 1.6% difference in acceptance. Measurements at the same center-of-mass energy are shifted slightly along the horizontal axis for clarity.

Other important diboson measurements are WZ in the fully leptonic channel with $WZ \to 3\ell\nu$ [16] and WV (where V is either W or Z) in the semileptonic channel $WV \to \ell\nu jj$ [17] with the boson decaying to quarks reconstructed as a single jet ("boosted" W/Z). For the fully leptonic channel, the cross section can be measured precisely, yielding $\sigma(pp \to WZ) = 48.09^{+2.98}_{-2.78}$ pb, in excellent agreement with the MATRIX NNLO prediction $\sigma_{\text{th}} = 48.98^{+1.08}_{-0.98}$. In the semileptonic channel, the background is too large to measure the full cross section. The WZ/WW final state, however, is the diboson final state most sensitive to WWZ couplings and limits on the anomalous triple gauge couplings (aTGC) can be set fitting the distribution of the diboson invariant mass m_{WZ}, as shown in figure 6 for a mass of

the "boosted" W/Z candidate between 65 and 105 GeV. This channel allows setting the most stringent limits on the coefficients c_{WWW}/Λ^2, c_W/Λ^2, and c_B/Λ^2 of dimension-6 EFT operators.

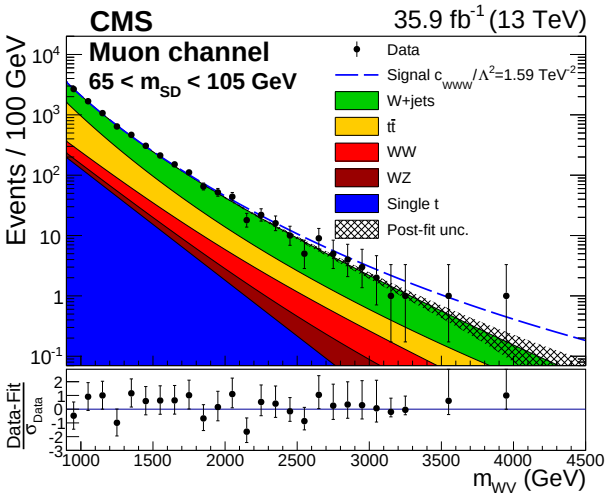

Fig. 6. Distribution of m_{WZ} in the signal region for the muon channel, with the result of the fit superimposed. An example of the excluded aTGC signal is represented by the dashed line [17].

Finally, WWW production has been searched for in the decay channels with three leptons or with two same-leptons and two jets [18]. The result $\sigma(pp \to WWW) = 0.17^{+0.32}_{-0.17}$ pb is one standard deviation lower than the SM expectation of $\sigma_{\text{th}} = 0.509 \pm 0.013$. The observed (expected) significance is 0.6 (1.78) and the upper limit on the signal is 0.78 pb, while 0.60 pb was expected in the case of no signal.

3.3. Vector boson scattering

The first observation of VBS has been reported in the WW same-sign leptons final state by CMS using proton–proton collisions data at 13 TeV collected in 2016 [19]. This final state has the largest ratio of EW signal to QCD background of all VBS processes. Background is mainly due to non-prompt leptons and WZ, and it is very low as can be seen in figure 7, where the distribution of tagging-jets invariant mass is shown. The observed (expected) significance of the signal is 5.5 (5.7) standard deviations. The measured fiducial cross section is $\sigma^{\text{fid}}_{W^\pm W^\pm} = 3.83 \pm 0.66(\text{stat.}) \pm 0.35(\text{syst.})$ fb in excellent agreement with SM: the ratio to the expected leading-order cross section is $\mu = 0.90 \pm 0.22$.

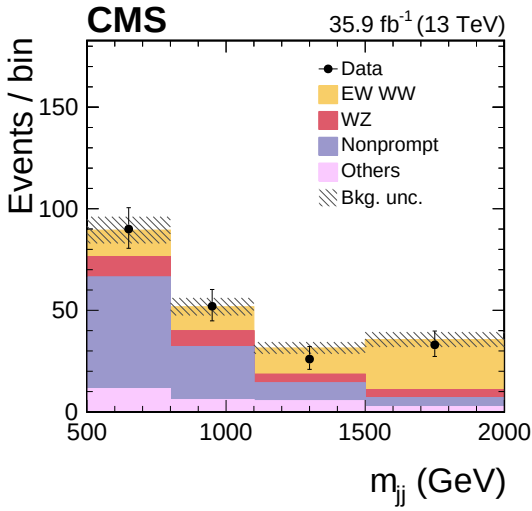

Fig. 7. Distributions of m_{jj} in the signal region. The normalization of the EW $W^{\pm}W^{\pm}$ and background distributions corresponds to the result of the fit. The hatched bands include statistical and systematic uncertainties from the predicted yields. The overflow is included in the last bin [19].

The VBS production of WZ in the fully leptonic final state, *i.e.* with three leptons, has been also measured with 2016 data [20]. The signal is extracted from a fit to the 2-dimensional distribution in invariant mass m_{jj} and pseudorapidity difference $|\Delta\eta_{jj}|$ of the tagging jets, as shown in figure 8. The result is in agreement with SM, with an observed (expected) significance of the EW signal of 2.2 (2.5) standard deviations, and a signal strength $\mu = 0.82^{+0.51}_{-0.43}$.

The final state with one W or Z boson decaying to leptons and another vector boson V decaying into quarks has been also investigated at 13 TeV [21]. Due to the large background from associated production of a vector boson and one or more jets, the sensitivity to SM cannot be achieved in this channel, but limits can be set to anomalous QGC (aQGC) from the distribution of invariant mass of WV and ZV, actually the most stringent bounds for these coefficients of dimension-8 EFT operators.

Some other coefficients can only be constrained by the ZZ or $V\gamma$ VBS channels. The VBS ZZ fully-leptonic final state has been also measured on the 2016 dataset at 13 TeV [22]. The result is consistent with the Standard Model, with a measured fiducial cross section $\sigma^{\text{fid}}_{ZZ} = 0.40^{+0.21}_{-0.16}(\text{stat.})\,^{+0.13}_{-0.09}(\text{syst.})$ fb and a signal strength $\mu = 1.39^{+0.86}_{-0.65}$, corresponding to an observed significance of 2.7 standard deviations (with 1.6 expected). The most stringent limits on EFT coefficients, however, are obtained from the $Z\gamma$ VBS production. A preliminary result using the same dataset is available

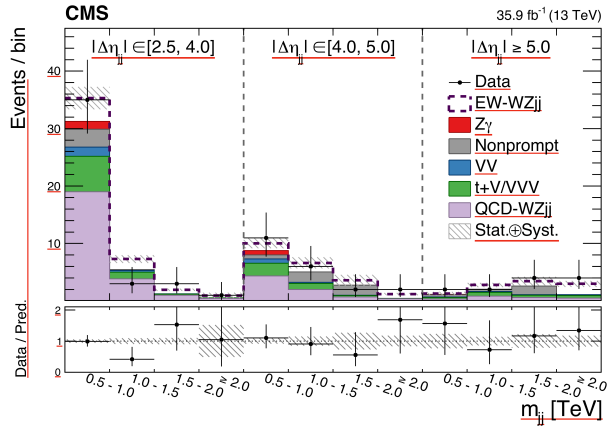

Fig. 8. The one-dimensional representation of the 2D distribution of m_{jj} and $|\Delta\eta_{jj}|$, used for the EW signal extraction. The x axis shows the m_{jj} distribution in the indicated bins, split into three bins of $|\Delta\eta_{jj}|$. The dashed line represents the EW WZ contribution stacked on top of the backgrounds that are shown as filled histograms. The hatched bands represent the total and relative systematic uncertainties on the predicted yields. The bottom panel shows the ratio of the number of events measured in data to the total number of expected events. The predicted yields are shown with their best-fit normalizations [20].

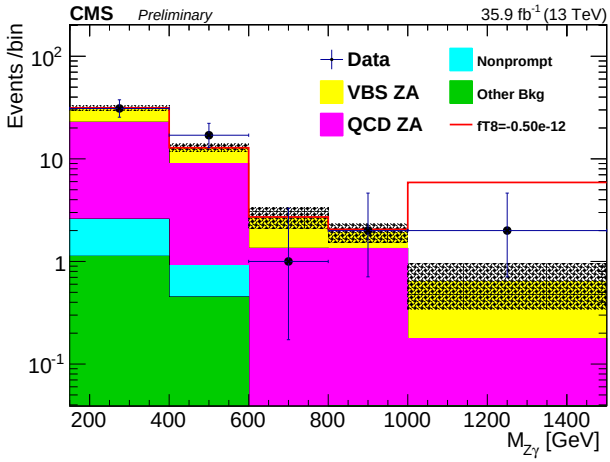

Fig. 9. (Color online) The $m_{Z\gamma}$ distribution of events satisfying the aQGC region selection, which is used to set constraints on the anomalous coupling parameters, that would significantly enhance the yields at high $m_{Z\gamma}$, as shown by the black/red line. The last bin includes overflow. The hatched bands represent the total uncertainties of the predictions [23].

for this channel [23]. The measured fiducial cross section is $\sigma^{\text{fid}}_{Z\gamma} = 3.20 \pm 0.07(\text{lumi.}) \pm 1.00(\text{stat.}) \pm 0.57(\text{syst.})$ with a signal strength $\mu = 0.64^{+0.23}_{-0.21}$. Combined with the Run 1 result on the same channel, this yields an observed significance of 4.7 standard deviations, with respect to 5.5 standard deviations expected. Figure 9 shows the distribution of $m_{Z\gamma}$ that is used to set limits on anomalous coupling parameters.

4. Summary

The most recent results obtained by the CMS experiment with Drell–Yan, W and multi-boson events have been presented. These allow fundamental tests of the SM, like measuring the electroweak mixing angle in DY events, and setting upper limits on the triple and quartic gauge couplings from the production of multi-bosons and from the EW production of vector bosons and jets. So far, no significant deviation from predictions has been found over more than nine orders of magnitude. This is an impressive test of the SM theory and very stringent bounds have been set on New Physics in the framework of EFT.

Nevertheless, we are now preparing for taking new data during Run 3, which will increase the amount of collected proton–proton interactions at the LHC up to 500 fb^{-1}. These new data will allow testing SM theory even further and might finally provide some evidence of New Physics.

REFERENCES

[1] CMS Collaboration, *JINST* **3**, S08004 (2008).

[2] CMS Collaboration, *J. High Energy Phys.* **1912**, 059 (2019).

[3] R. Gavin, Y. Li, F. Petriello, S. Quackenbush, *Comput. Phys. Commun.* **182**, 2388 (2011).

[4] CMS Collaboration, *J. High Energy Phys.* **1912**, 061 (2019).

[5] CMS Collaboration, *Eur. Phys. J. C* **78**, 701 (2018).

[6] CMS Collaboration, «A proposal for the measurement of the weak mixing angle at the HL-LHC», CMS-PAS-FTR-17-001, 2017, `http://cds.cern.ch/record/2294888`.

[7] S. Alioli, P. Nason, C. Oleari, E. Re, *J. High Energy Phys.* **0807**, 060 (2008).

[8] R.D. Ball *et al.*, *J. High Energy Phys.* **1504**, 040 (2015).

[9] K. Hagiwara, S. Ishihara, R. Szalapski, D. Zeppenfeld, *Phys. Rev. D* **48**, 2182 (1993).

[10] C. Degrande *et al.*, *Ann. Phys.* **335**, 21 (2013).

[11] CMS Collaboration, *Eur. Phys. J. C* **80**, 43 (2020).

[12] M. Bahr *et al.*, *Eur. Phys. J. C* **58**, 639 (2008).

[13] CMS Collaboration, «Measurement of the $pp \to ZZ$ production cross section at $\sqrt{s} = 13$ TeV with the Run 2 data set», CMS-PAS-SMP-19-001, 2019, http://cds.cern.ch/record/2668717.

[14] M. Grazzini, S. Kallweit, M. Wiesemann, *Eur. Phys. J. C* **78**, 537 (2018).

[15] J.M. Campbell, R. Ellis, *Nucl. Phys. B Proc. Suppl.* **205–206**, 10 (2010).

[16] CMS Collaboration, *J. High Energy Phys.* **1904**, 122 (2019).

[17] CMS Collaboration, *J. High Energy Phys.* **1912**, 062 (2019).

[18] CMS Collaboration, *Phys. Rev. D* **100**, 012004 (2019).

[19] CMS Collaboration, *Phys. Rev. Lett.* **120**, 081801 (2018).

[20] CMS Collaboration, *Phys. Lett. B* **795**, 281 (2019).

[21] CMS Collaboration, *Phys. Lett. B* **798**, 134985 (2019).

[22] CMS Collaboration, *Phys. Lett. B* **774**, 682 (2017).

[23] CMS Collaboration, «Measurement of electroweak production of Z gamma in association with two jets in proton–proton collisions at $\sqrt{s} = 13$ TeV», CMS-PAS-SMP-18-007, 2019, http://cds.cern.ch/record/2682214.